Four-Leaf-Clover-Shaped EBG Structure to Improve the H/E Field Ratio of Stripline Coil for 7 Tesla MRI

Gameel Saleh[1], Klaus Solbach[1], Daniel Erni[2], and Andreas Rennings[2]
[1]High-Frequency Technique (HFT), [2]General and Theoretical Electrical Engineering (ATE)
University of Duisburg-Essen, and [2]CENIDE – Center for Nanointegration Duisburg-Essen,
47048 Duisburg, Germany

***Abstract*—This paper presents a multilayer four-leaf-clover-shaped EBG structure as a high impedance surface behind a 7 Tesla MRI stripline coil (meander dipole), operating at 300MHz. The proposed EBG structure has been characterized by its in-phase band gap reflection coefficient, and the surface wave suppression band gap properties. The electrical cell size of the analyzed EBG structure has been reduced to 6.8% of free-space wavelength. The MRI strip-line coil backed by the proposed EBG structure exhibited stronger (by 57%) magnetic over electric field ratio than the original design using a PEC ground plane for the coil. The longitudinal RF field of view (FOV) has been maximized when the strip-line coil length is increased from 25cm to 35cm.**

Index Terms – electromagnetic band gap (EBG) structures; magnetic resonance imaging (MRI); in-phase reflection band; surface wave suppression band gap; specific absorption rate (SAR).

I. INTRODUCTION

The anti-phase currents in the metallic conductor (PEC) ground plane placed underneath a stripline transmit element for high field MRI, represents the main reason for the reduction in RF magnetic flux density above these coils (inside the phantom). The objective of this paper is to replace this PEC ground plane by a high impedance surface-EBG structure [1] to improve the efficiency of a well-established strip-line coil [2]. The EBG structure suppresses the anti-phase currents, when its stop band gap is properly achieved, whereas its in-phase band gap reflection coefficient satisfies the artificial magnetic conductor (AMC) like condition. Thereby, the magnetic flux density inside the phantom is increased. In this paper, a multilayer EBG structure with four-leaf-clover- shaped patches was used as a size-reduced solution compared to the solid geometry in [3]. The unit cell dimensions of the proposed EBG structure is shown in Fig. 1, with a lateral cell size of 6.8% of the free-space wavelength (λ_{300MHz}) instead of 7.5% in [3], and less than one-half of the substrate thickness as used in [4].

II. PROBLEM FORMULATION AND DESIGN SPECIFICATIONS

For a plane wave illuminating symmetric EBG surface at normal incidence, the structure can be modeled analytically by using the simple parallel LC resonant circuit formalism [1]:

$$\omega_0 = \frac{1}{\sqrt{LC}} \quad (1); \qquad Z = \frac{j\omega L}{1-\omega^2 LC} \quad (2)$$

where ω_0 is the angular resonance frequency and Z is the surface impedance of the EBG structure. The values of the capacitance C and the inductance L are determined in [1].

The proper EBG structure follows a multilayer design encompassing two arrays of metal patches diagonally offset from each other. The top layer consists of slotted patches (four-leaf-clover) of 6.8% of λ_{300MHz}, connected to the metal backed dielectric substrate by vertical pins. The lower layer consists of solid patches of 6% λ_{300MHz}, and is floating. The HFSS full wave simulator, based on the FEM algorithm and the FDTD simulator EMPIRE XCcel were used to characterize and analyze the EBG structure. The geometry of the proposed EBG structure together with a resonant meander dipole printed on FR4 epoxy over the EBG structure is shown in Fig. 1.

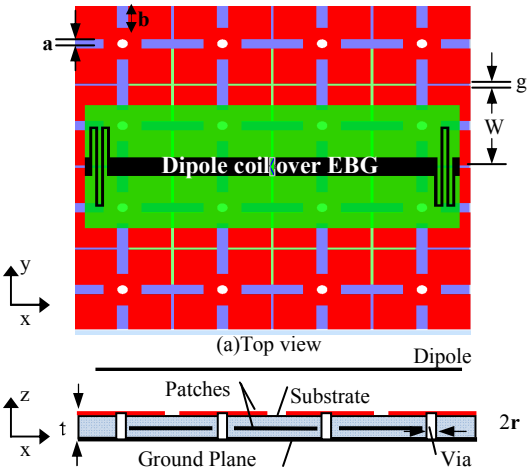

(b) Cross section view of the proposed EBG structure

Figure 1. Offset layers stacked EBG design with a meandered dipole

The physical dimensions of the proposed EBG structure are

$W = 0.068\ \lambda_{300MHz}$, $g = 0.002\ \lambda_{300MHz}$, $t = 0.0064\ \lambda_{300MHz}$, $r = 0.0035\ \lambda_{300MHz}$, $a = 0.008\ \lambda_{300MHz}$, and $b = 0.02067\ \lambda_{300MHz}$. (3)

where λ_{300MHz} is used as a reference length, W is the patch width, g is the gap width, a is the slot width and b is the slot length and t is the thickness of two Arlon AR-1000 substrates, with a relative dielectric constant of 10.9. The spacing between the two layers of patches was chosen to be 0.0032 λ_{300MHz} due to the availability of laminates of 3.2mm thickness. This diagonally offset multilayer design provides more coupling between the adjacent patches. Thus, it is more capacitive, and

978-88-907018-1-8/13/$31.00 ©2013 IEEE

operates at lower frequency than the conventional single layer mushroom EBG structure, and the EBG structure with double layers representing the same boundary condition, as introduced in [4].

III. Reflection Phase Property

Fig. 2 compares the reflection phase of the proposed EBG structure and the solid patches geometry used in [3], both with the same patch width size (0.075 λ_{300MHz}). The frequency corresponding to zero degree reflection phase of the proposed slotted EBG structure is shifted down from 300MHz to 275MHz. This result is due to the slots in the new geometry which elongate the path through which the currents pass. Thus, the surface becomes more inductive. The existence of these slots, enabled us to miniaturize the patches width to 68mm, such that the frequency corresponding to zero degree reflection phase is shifted up to the MRI operating frequency of 300MHz. Thus the structure works as an artificial magnetic conductor with the aim of maximizing the field ratio inside the phantom. Within this geometry, 4×6 unit cells instead of 3×5 (60% more) could be used with the same substrate size (28cm×42cm) as in [3]. For miniaturization purposes, only 4×4 unit cells have been used with a dimension of 28cm×28cm.

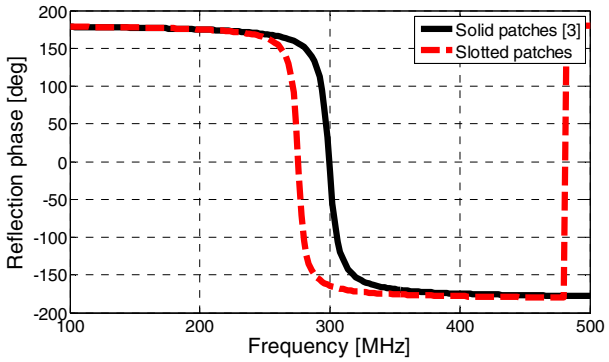

Figure 2. Reflection phase of the proposed and reference EBG structure

IV. Stop Band Gap Property

In this section, the effects of the number of unit cells on the stop band gap property of the proposed EBG structure are investigated using direct transmission method [5]-[6]. In this method, a two-port waveguide is formed by two electric walls (PEC) and two magnetic walls (PMC) shown in Fig. 3.

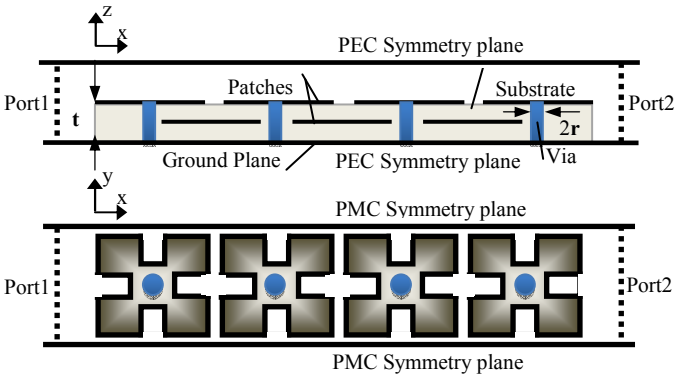

Figure 3.Simulation model of direct transmission method

The unit cells are centered in the waveguide along the x-axis. It is a TEM waveguide with boundary condition that has no cutoff frequency. The input wave is excited at port1 in free space and at normal incidence. The direction of propagation is from left to right.

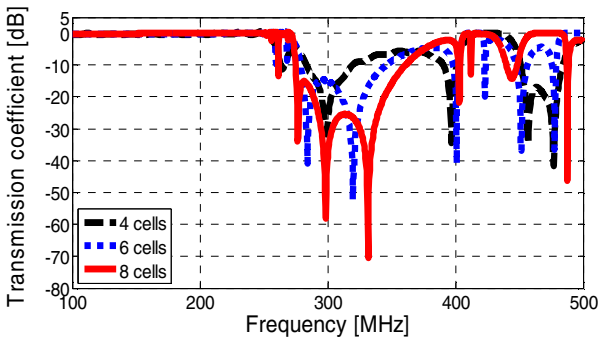

Figure 4. S_{21} parameter of the proposed EBG structure with various cell numbers in a row, using the direct transmission method.

Fig. 4 shows the transmission coefficient of the proposed EBG structure for various numbers of cells in the longitudinal direction yielding a wider stop band for an increasing number of unit cells. This figure also confirms that the MRI operating frequency is located within this stop band gap (determined by -10dB criteria) for the different numbers of cells.

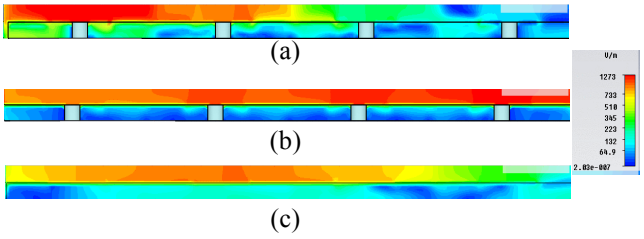

Figure 5. Electric field distribution (a) at 300MHz (inside the stop band gap), (b) at 200MHz – outside the stop band gap, and (c) at 300 MHz in the absence of vias (no band gap)

In Fig. 5a, time stepped animation over the entire phase cycle shows the attempts of the waves to propagate through the waveguide at frequencies inside and outside the designed stop band gap (the band gap through which the surface waves are suppressed). The electric field distribution in Fig. 5a shows the unsuccessful propagation of surface waves at the MRI operating frequency, 300MHz, which lies within the stop band gap. Due to the presence of the vias, the vertical electric field causes currents to flow and link between the surfaces, and provides the impedance of a parallel resonant circuit. This interaction between the vias and the electric field causes the electric field to slowdown and fits inside the structure and stops of propagation.

Fig. 5b shows for any other frequency, as 200MHz, which is beyond the stop band gap, the resonant behavior of the EBG structure is not excited, and energy can propagate in the waveguide from the left port to the right one. Fig. 5c shows the electric field distribution in the absence of the vias, where the surface waves propagate and the structure behaves like a metal backed dielectric slab.

V. The Ratio of Magnetic over Electric Field Inside the Phantom and Field of View (FOV)

With respect to the dominant problem of SAR in high-field MRI, the performance of the original coil configuration based on a stripline coil over a PEC ground plane was compared in a fair manner to the performance of the design using the EBG structure as a ground plane by simulating the distribution of magnetic over electric field ratio 4cm inside a homogeneous phantom ($\varepsilon_r = 40$, $\sigma = 0.8$ S/m) placed 2cm above the coil. The entire height of the coil and the PEC or EBG structure is kept constant to 3.4cm. In Fig. 6, the 25cm stripline coil backed by the proposed EBG structure exhibits a stronger $|H|/|E|$ than the original design when the RF coil was backed by a PEC [2]. The maximal improvement in this ratio reaches to 57%.

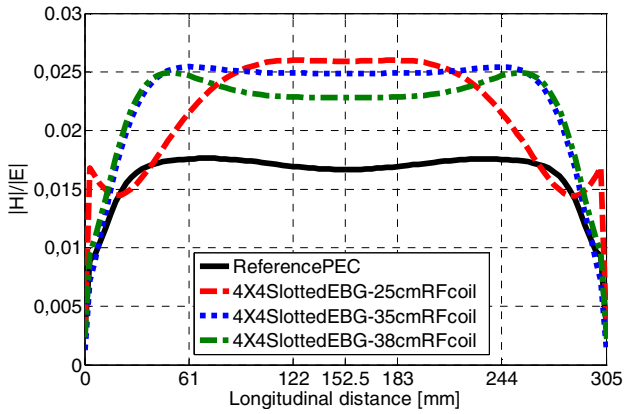

Figure 6. FDTD longitudinal distribution of magnetic over electric field ratio for the 25cm stripline coil backed by the reference PEC, and for different RF coil lengths backed by the proposed slotted EBG structures.

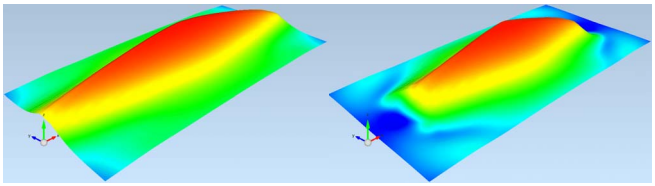

(a) (b)

Figure 7. Magnetic field H_y distribution in air at 1cm above the RF dipole (a) for the 35cm element (b) for the 25cm element. (FDTD simulation with EMPIRE)

In Fig. 6 and 7, the RF field of view is maximized when the dipole length is increased, from 25cm to 35cm. Thus the expensive scanner time in MRI is minimized.

VI. Conclusion

In this work, a multilayer four-leaf-clover-shaped EBG structure with a miniaturized electrical cell size of 6.8% of λ_{300MHz} has been utilized. The analyzed EBG structure satisfied the AMC reflection coefficient property with MRI operating frequency corresponding to a zero degree reflection phase. The operating frequency is also located within the useful stop band gap through which the surface waves ceases to propagate. The more the number of cells, the wider the stop band gap is. The MRI strip-line coil backed by the proposed EBG structure exhibited stronger (by 57%) magnetic over electric field ratio than the original design using a conventional metallic ground plane for the coil. The longitudinal RF field of view (FOV) has been maximized when the strip-line coil length is increased from 25cm to 35cm.

References

[1] D. Sievenpiper, High-impedance electromagnetic surfaces, PhD dissertation, Dept. Elect. Eng. Univ. California at Los Angeles, Los Angeles, CA, 1999.

[2] S. Orzada et al., Proc. Intl. Soc. MRM 16 (2008), p.2979

[3] G. Saleh, K. Solbach, and A. Rennings, EBG structure to improve the B1 efficiency of stripline coil for 7 Tesla MRI, EuCAP 2012, Prague, March 2012.

[4] G. Saleh, K. Solbach, and A. Rennings, EBG Structure for Low Frequency Applications, GeMiC 2012, Ilmenau, March 2012.

[5] R. Remski, Analysis of PBG surfaces using Ansoft HFSS, Microwave J 43 (2000), 190–198.

[6] L. Liang, C.H. Liang, L. Chen, X. Chen, Anoval broadband EBG using cascaded mushroom-like structure, Microwave and Optical Technology Letters Volume 50, Issue 8, pages 2167–2170, August 2008.